

IMPROVING COSMIC RAY COMPOSITION DETERMINATION THROUGH BETTER TRACKING

O. Ganel and E.S. Seo

Institute for Physical Science and Technology, University of Maryland, College Park, MD 20742, USA

ABSTRACT

Several experiments now under construction or in various stages of study are intended to improve cosmic ray composition measurements through element (or element group) identification. To achieve this, some form of finely segmented (pixel) charge detector will be used to reduce the effects of back-scattered particles on the measurement. These experiments will utilize ‘tracking calorimeters’ to reconstruct the trajectory of high-energy cosmic particles through the charge measurement device to identify the correct pixel. As an example, the Advanced Cosmic-ray Composition Experiment on the Space Station, a mission currently being studied, is aimed at obtaining more precise measurements, above the atmosphere, of the element-by-element (H – U) fluxes of cosmic ray particles at the limiting energies expected from supernova shocks. The expected energy reach is 10^{15} eV for H – Fe but less than 10^{10} eV for the heavier nuclei, which do not depend on the calorimeter. The following describes a tracking algorithm based on information from the calorimeter, scintillators, and charge detector, suggests some design choices, and estimates the expected tracking resolution for this experiment.

INTRODUCTION

When a high-energy proton (or nucleus) enters a thick block of matter it undergoes a nuclear interaction, generating a large number of secondary particles (mostly π^+ , π^- , and π^0), which carry off a large fraction of its energy. The π^0 's decay almost immediately into pairs of photons, which then initiate electromagnetic (EM) showers or cascades (large collections of electrons, positrons, and photons). The surviving primary and charged secondaries travel some distance deeper into the block before undergoing further nuclear interactions. This hadronic/EM cascade continues until the shower particles possess relatively low energies, at which point other processes begin to dominate and the shower energy is absorbed. The overall shape of a hadronic shower thus has a relatively narrow (several cm typical radius) EM core, surrounded by a (typically order of magnitude) wider halo of soft hadronic activity.

Mass limitations preclude space-based calorimeters of sufficient depth for full shower containment. Instead, these experiments may have a carbon target to force nuclear interactions and sufficient depth to contain enough of the EM cascades generated in the first interaction to measure the primary energy. The relative thinness of such calorimeters has several implications. First, large, non-Gaussian fluctuations in the EM energy fraction of the first interaction limit the energy resolution of such a device to about 35% – 40%. Second, since this EM fraction is almost energy independent, the device provides an almost linear response to hadrons, making data interpretation relatively simple. Finally, the geometry factor is obviously greater for thinner devices of equal lateral dimensions.

The baseline design of the Advanced Cosmic-ray Composition Experiment on the Space Station (ACCESS), shown in Figure 1, includes a charge measurement section (UH) capable of resolving individual nuclei (H – U), a Transition Radiation Detector (TRD) for velocity measurement, and a calorimeter for energy measurement. The calorimeter section is comprised of a silicon matrix charge detector (Si), a thick carbon target interleaved with several pairs of crossed scintillator strip trigger planes, and a Bismuth Germanate (BGO) calorimeter with laterally

oriented crystals in crossed layers. The target will force nuclear interaction in more than 63% of incident protons (and larger fractions for heavier nuclei). Calorimetry is the only practical method to measure the energy of protons and He nuclei at the high energies necessary to look for the proton spectral break hinted at by existing data (Asakimori *et al.*, 1993). ACCESS should also be able to verify if the spectral indices for protons and He nuclei are indeed different, hinting at different acceleration mechanisms.

THE ROLE OF TRACKING

Besides measuring energy, the segmented ACCESS calorimeter will ‘track’ the shower axis, allowing reconstruction of the incident particle’s trajectory. The reconstructed track can then be used to identify the pixel crossed by the incident particle, allowing charge identification. Charge detector segmentation will reduce the overlay of back-scattered shower particles believed to have caused high-energy protons to be misidentified as He nuclei, thereby distorting the two species’ measured spectra (Ellsworth *et al.*, 1977).

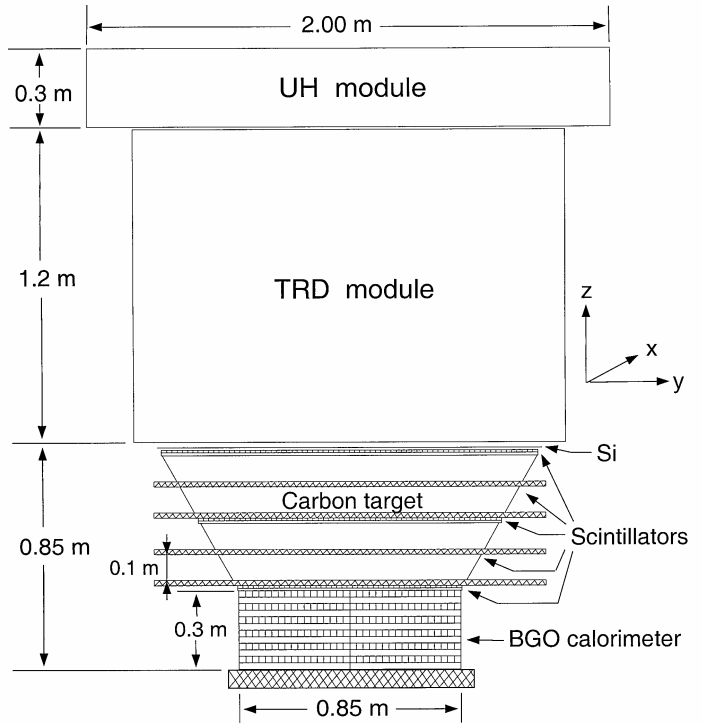


Fig. 1. Schematic of baseline ACCESS design

Reliable tracking is required for the charge detector to properly identify which of the numerous hits in a typical high-energy event was caused by the incident particle. It is unfortunate that shower axis reconstruction accuracy is strongly energy dependent. At low energies the angle between the incident direction and the direction of any given secondary can be quite large. Low energy EM cascades are also rather shallow, i.e., absorbed in a relatively short distance, providing few points for fitting and making slope determination less accurate (the impact of this could be ameliorated by finer BGO segmentation, e.g. 1.0 cm rather than the baseline design’s 2.5 cm). These effects lead to poorly measured, wider shower cores, with large angles possible between the reconstructed track and the real trajectory. These uncertainties are exacerbated by the long extrapolation distance needed up to the Si matrix (about 50 cm from the top of the BGO), or worse yet, to the UH module at the top of ACCESS (170 cm).

At high energies, the shower core lies along the shower axis, but many more back-scattered shower particles confuse the charge measurement, so excellent resolution is needed. Previously (Seo *et al.*, 1996), a calorimeter-based algorithm was suggested as a solution to this requirement. Studying simulated events at various energies, and with different detector configurations, we have developed an algorithm that utilizes information from the target scintillator strips and the Si matrix, in addition to the BGO calorimeter energy deposit pattern.

TRACKING ALGORITHM

We studied events where a proton, incident on the top surface of the detector undergoes a nuclear interaction in the carbon target or the top 5 cm of the BGO, and the incident particle trajectory exits the calorimeter after at least six layers of BGO (15 cm). We also required that the event pass certain trigger requirements, i.e., produce certain signals in the (1.0 cm wide) strips of the scintillators and BGO crystals. At least 1.5 MeV was required to be deposited in at least one strip of the top and bottom scintillator planes. At least one BGO crystal in each layer had to have at least 50 MeV deposited (twice the mean minimum ionizing particle signal), or four or more layers had to each contain a crystal with a 1 GeV or higher energy deposit. For these events we derived BGO-only and BGO + scintillator + Si fits, separately in the x-z and the y-z planes. Each fit required at least 3 BGO points.

For both fit types, we first calculated average (centroid) positions in each BGO layer, weighted with the square of the crystal energy deposits. We excluded crystals with less than 10% of the highest deposit in their layer, layers with less than 3% of the total BGO deposit, and layers in which the highest deposit was in an edge crystal. This last indicates that a major part of the shower leaked out the side, which would bias the position determination. Each

layer point was weighted with the inverse of its deposit pattern RMS width. For the BGO + scintillator + Si fit, we then selected the Si pixel hit providing the best fit (smallest χ^2/dof , where dof is the number of degrees of freedom in the fit) with the BGO points. Hit pixels were considered if they were, fully or partially, within 3σ of the extrapolated BGO fit point, in terms of the uncertainty of its location.

Next, we turned to the target scintillator layers. Here we differentiated between those layers below the shower starting point and those above it. Any layers below the starting point were treated in the same manner as the BGO layers (energy-squared-weight centroid in the layer, inverse of pattern-width as weight in the linear track fit).

Scintillator layers above the shower starting point will register only the primary track and whatever back-scattered particles result from the shower. Since a centroid in such layers will not necessarily reproduce the primary track position, the strategy here was to look for single hits in the 3σ area defined above. All possible combinations of a single hit in each such layer (or no hit, if a good hit was not found) were combined with the points below the start of the shower. Each hit was assigned a weight equal to the average weight of the centroid points. We selected the combination with the most points and $\chi^2/\text{dof} < 1$, or if such did not exist, the combination with the smallest χ^2/dof .

In those cases where the track fit using all BGO, scintillator, and Si information had a greater χ^2/dof than the BGO-only fit, and/or if the former had a χ^2/dof value greater than unity, the point most out of agreement with the track was removed from the fit. In those events where the reconstructed track pointed at a cluster of hits produced by back-scattered particles, the fit was as likely to suffer from the additional hit as it was to benefit from it. Thus, if a scintillator hit selected above the shower starting point had another hit within 2 cm, that layer was removed as well.

RESULTS AND DESIGN IMPLICATIONS

Figure 2 shows the extrapolation accuracy at the top of the target for 1 TeV protons incident isotropically from the upper hemisphere, at random positions, with 5 scintillator layer pairs of 1 cm wide strips. The resolution is shown both for (a) the BGO-only fit and for (b) the fit using BGO and scintillators. Note that the latter predicts a position at the top of the target within 3 mm (σ) of the true position, as determined by the Monte Carlo information. This is better, on average, by a factor of 7 when compared to the BGO-only fit. Charge measurement is not possible for events with no hit in the top layer, so such events were not considered.

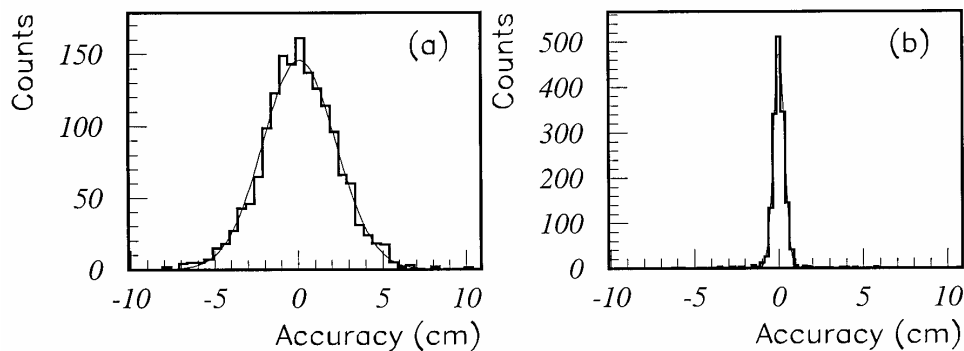


Fig. 2. Extrapolation accuracy at top of target for 1 TeV protons for (a) BGO-only and (b) BGO + scintillator fits.

Figure 3 plots the extrapolation resolution at the top of the target as a function of target scintillator strip-width. Note that the resolution scales roughly as $d/\sqrt{12}$, where d is the strip-width, as expected for digital hits (equalizing areas under Gaussian and square-shape distributions). The fact that the scaling is not exact is due to the combination of single-hit and centroid treatment of scintillator layers, and to the use of the linear fit. As the strip-width increases, the improvement due to the scintillators decreases, disappearing at a width of 7 cm. An optimal design would match the ‘confusion circle’ (a 3σ circle around the track in which the primary is nearly certain to have entered) diameter to the Si pixel size. By this measure, 1 cm wide scintillator strips seem well matched to $2 \times 2 \text{ cm}^2$ Si pixels.

Next, we deal with the question of how many scintillator layers ACCESS should use. For about half of all selected events two layers might be sufficient (indeed, for 10% of all events the BGO-only fit is good enough). For the other half, however, one layer might have fluctuated below the threshold, while another one or two could have been

removed from consideration by the algorithm described above. Naturally, the removal of scintillator layers pulls a non-negligible fraction of events back to the level of BGO-only resolution. If, however, there is no choice in the matter, the damage is least when (counting from top (1) to bottom (5)) layer 4 is removed, and then layer 3. This strategy keeps the top layers, where most events will have single hits, thereby minimizing the extrapolation uncertainty. Layer 5 is kept for triggering purposes.

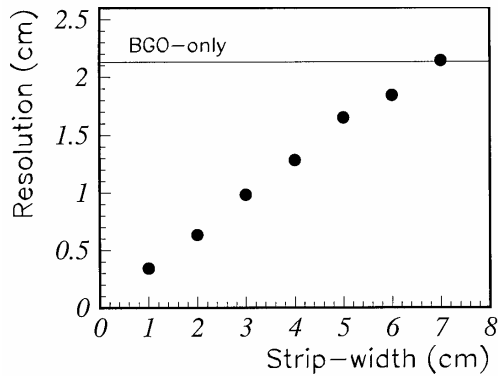


Fig. 3. BGO + scintillator extrapolation resolution at top of target for 1 TeV protons vs. strip width.

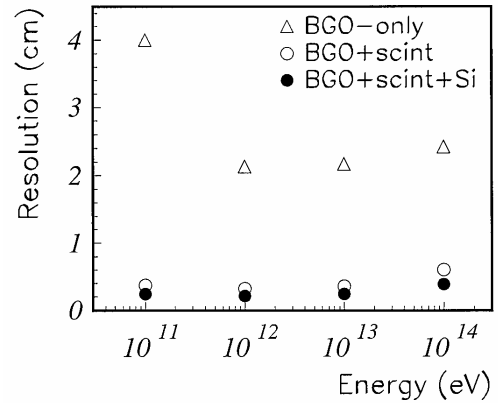


Fig. 4. Extrapolation resolution at top of target vs. proton energy.

EXPECTED PERFORMANCE

As shown in Figure 4, a simulated ACCESS configuration with five layers of 1 cm wide scintillator strips provides a 4 – 6 mm (nearly energy independent) extrapolation resolution for $10^{11} - 10^{14}$ eV protons (empty circles). Adding a Si matrix provides a 34% improvement (scaled from a simulated configuration including a Si matrix) leading to a resolution of 3 – 4 mm over that range of energies (full circles). This is to be compared with the poorer, and energy dependent, BGO-only extrapolation resolution (empty triangles). At a height of 170 cm above the calorimeter, where the ACCESS UH module will be located, the extrapolation uncertainty would increase, due to a longer extrapolation length, to about 14 mm (confusion circle diameter of 8 cm). Using the Si information should reduce this to about 5 cm. Accordingly, the segmentation of the UH module should not be larger than about 5×5 cm².

CONCLUSIONS

We suggest a track reconstruction algorithm utilizing calorimeter, scintillator, and Si pixel information in, e.g., ACCESS. With five layer pairs of 1 cm wide scintillator strips and a Si matrix with 2×2 cm² pixels, this algorithm should allow sufficiently accurate identification of the primary particle's incident position for charge measurement to be performed on the correct particle. This resolution should be almost energy independent up to 10^{14} eV. Events with a high density of backward scattered shower particles near the primary trajectory can be flagged. The algorithm can be tuned separately for this class of events, more common at high energies. Further studies will be carried out to suggest design choices to ameliorate the hit density problem, which may require finer segmentation.

ACKNOWLEDGEMENT

This work was supported by NAG5-5155.

REFERENCES

- Asakimori, K., T.H. Burnett, M.L. Cherry, M.J. Christi, S. Dake, *et al.*, Cosmic Ray Composition and Spectra: Protons, *Proceedings of the 23rd International Cosmic Ray Conference (Calgary)*, **2**, 21, (1993).
- Ellsworth, R.W., A. Ito, J. MacFall, F. Siohan, R.E. Streitmatter, *et al.*, On the High Energy Proton Spectrum Measurements, *Astrophysics and Space Science*, **52**, 415, (1977).
- Seo, E.S., J.H. Adams Jr., G.L. Bashindzhagyan, O.V. Dudnik, A.R. Fazely, *et al.*, The Advanced Thin Ionization Calorimeter (ATIC) Balloon Experiment: Expected Performance, *Proceedings of SPIE (Colorado)*, **2806**, 134, (1996).